Supporting information for

Chemically non-perturbing SERS detection of catalytic reaction with black silicon

E. Mitsai, A. Kuchmizhak, E. Pustovalov, A. Sergeev, A. Mironenko, S. Bratskaya, D.P. Linklater, A. Balčytis, E. Ivanova, S. Juodkazis

March 4, 2018

Contents

1 Synthesis of the Ag nanoparticles.

Silver nanoparticles were prepared by the reduction of silver nitrate (99%, Sigma-Aldrich) solution with sodium citrate. Briefly, 8 ml of $2.5{\cdot}10^{-4}$ M $AgNO_3$ water solution was heated to boiling point, then 2 ml of 0.025% potassium citrate solution was added dropwise under vigorous steering. The solution was kept stirring at about 30 min until a yellow-brown color change was observed, then cooled down to room temperature and dialyzed for 12 h against distilled water using 3.5 kDa dialysis membrane (Orange Scientific) to remove excess of the citrate. Obtained particles were characterized by transmission electron microscopy using Carl Zeiss Libra 200 microscope at an accelerating voltage of 80 kV demonstrating the near spherical shape and diameter ranging from 5 to 10 nm (Fig. S1).

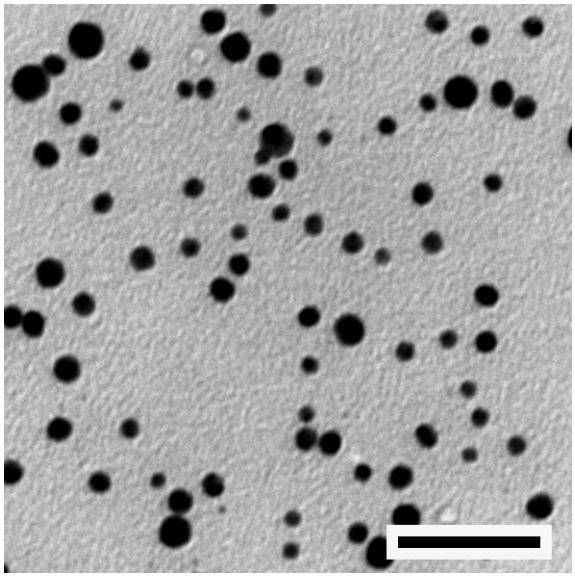

Figure 1: TEM image of Ag nanoparticles. Scale bar corresponds to 50 nm.

2 Back-scattering spectra of the isolated spiky Si resonators of various size.

Here, we show the FDTD calculations of back-scattering spectra from the isolated spiky Si structures placed onto the bulk Si substrate to indicate the excitation of various size-dependent Mie resonances. The spiky structures are modeled to have the variable height ranging from 200 to 500 nm and the fixed taper angle of 25^o, which is in agreement with the real surface textures under study. The spectrally broadband total-field scattered-field source was used to normally irradiated the structures. Figure S2 shows normalized back-scattering spectra calculated for spiky Si Mie resonators of variable size. The red-shift of the main dipolar-like mode is clearly observed upon increasing the height of the spiky feature from 200 to 500 nm. Appearance of the high-order resonances in the scattering spectra can be identified for spikes with height exceeding 300 nm. The characteristic H-field distributions in the insets calculated in the xy plane for the certain structures under resonant wavelength illustrate the excitation of dipolar and quadrupolar like magnetic-type modes. Note the magnetic- and electric-type dipolar modes are spectrally overlapped owing to the effect of the underlying high-index substrate. Importantly, the presented calculations demonstrate that the high-dense arrangement of the tipped structures on the substrate as well as the size deviation of the isolated spikes ensures the broadband response of the substrate allowing operation at various excitation wavelength.

3 Temperature-dependent Raman band of the crystalline silicon for bare and metal-coated black silicon substrates.

Along with the substantially enhanced EM field near the surface of such resonator, this gives an additional modality to the chemical SERS measurements allowing in-situ detection of the local temperature of the resonator via tracking the spectral shape and position of the temperature-dependent c-Si Raman band, which can be resonantly excited within the Si resonator. In the range of applied intensities used for Raman measurements (12-

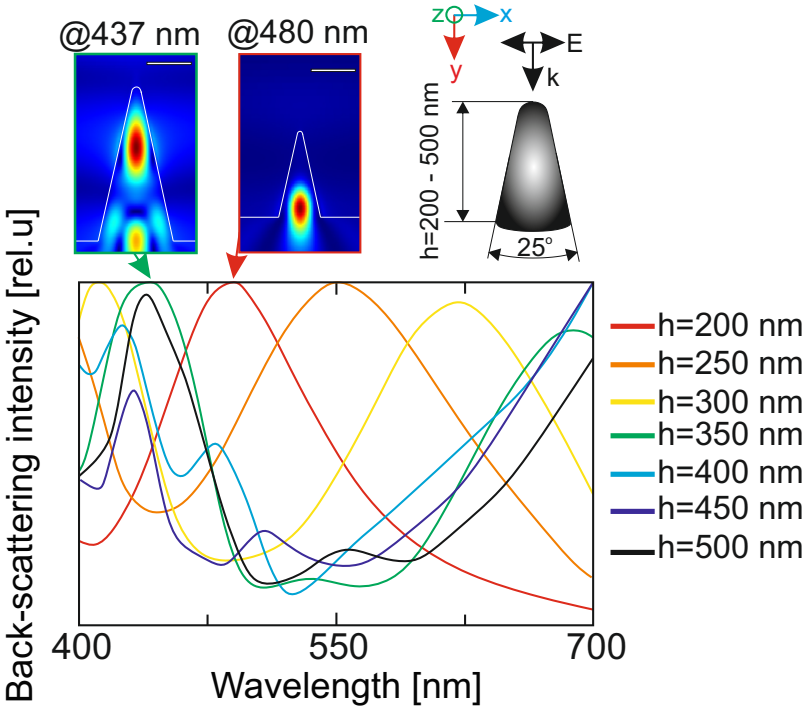

Figure 2: Normalized back-scattering spectra calculated for isolated spiky Si resonators of variable height h ranging from 200 to 500 nm. The insets explain the calculated geometry and provide characteristic H-field distribution obtained under resonant excitation of a certain structures.

120 μW/μm^2), we did not observe any substantial variations of the shape and position of the c-Si band for bare black silicon substrate (Fig. S3(a)). As shown, small detectable spectral shift of the c-Si band is observed only for much higher intensity of 37.6 mW/μm^2, indicating potentially weak contribution of the temperature effect to the SERS data presented in the manuscript. Additionally, we also attested the silver-coated b-Si substrates showing the shift of about 1 cm^{-1} already at 120 μW/μm^2 (Fig. S3(b)), which corresponds to small temperature increase of ΔT=50 K according to the previous estimations. More efficient heating of the metal-coated substrates can proceed via the plasmon-assisted mechanism. Additionally, the b-Si coated with a 100-nm thick Ag film demonstrates no detectable c-Si Raman band even under higher excitation intensity, potentially indicating complete coverage of the Si surface with the metal film (Fig. S3(b)).

4 Comparison of the PATP-to-DMAB reaction rates for the silver- and gold-coated black silicon.

Here, we provide the comparative study of the SERS enhancement and PATP-to-DMAB conversion rate measured on the b-Si substrate coated with Ag and Au films having the same thicknesses of 20 nm. Figure S4(a) shows the comparative time-resolved SERS spectra of the PATP (at molar concentration of 10^{-6}) coated on the Au-(bottom) and Ag-coated (top) b-Si substrates. Being compared to the Au/b-Si, the silver-coated substrate provides an order of magnitude higher SERS yield, allowing to use an order of magnitude lower excitation intensity of 13 μW/μm^2 to clearly track the PATP-to-DMAB conversion.

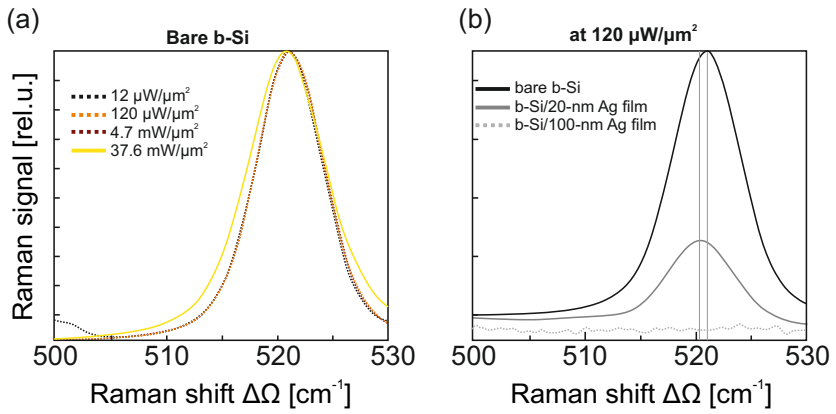

Figure 3: (a) Raman spectra near the temperature-dependent c-Si band obtained under irradiation of the bare b-Si at various excitation intensities. (b) Similar Raman band obtained for bare and silver-coated b-Si at excitation intensity of 120 μW/μm^2. Each presented spectrum is averaged over 20 similar measurements.

Analysis of the time evolution of the DMAB Raman band at 1432 cm^{-1} in the obtained SERS series allows to access the PATP-to-DMAB conversion versus the laser irradiation time (Fig. S4(b)). As seen, for the fixed initial concentration of the PATP molecules in solution of 10^{-6} M deposited onto the substrates pre-coated with Au and Ag films, chemically active silver provides an order of magnitude faster conversion rate being compared to the Au coating taking into account different laser irradiation intensity (Fig. S4(b)).

5 Comparison of the PATP-to-DMAB conversion on the Ag-coated b-Si for dried PATP layer and for PATP in the aqueous methanol solution.

Here, we present the measurements of the PATP-to-DMAB conversion performed in the aqueous methanol solution of the PATP on the Ag-coated b-Si (the Ag film thickness is 100 nm) in comparison to the measurement of the dried PATP layer on the similar substrate (see Methods). As seen, the Ag/b-Si in the methanol solution maintains relatively fast PATP-to-DMAB conversion similar to those obtained from the dried layer. For both measurements, the conversion occurs within the 60 seconds of irradiation. Noteworthy, the addition of the colloidal silver to the PATP solution does not cause any substantial variation of the conversion rate on the Ag/b-Si substrate.

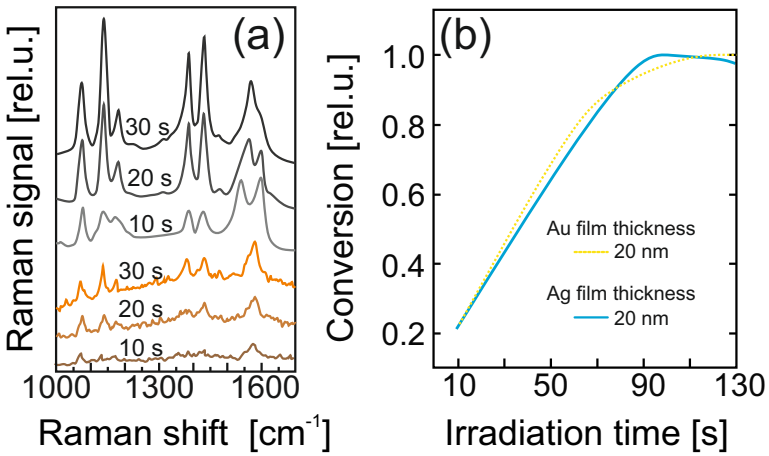

Figure 4: (a) Time-resolved SERS spectra of the PATP layer adsorbed on the Au-coated (three bottom curves) and Ag-coated (three upper curves) b-Si substrates. Both metal coatings have the thickness of 20 nm. The total irradiation time of the PATP molecules is indicated near each spectrum, while the accumulation time for each spectrum is 10 s. (b) PATP-to-DMAB conversion versus laser irradiation time. The conversion is defined as a normalized intensity of the DMAB characteristic Raman band at 1432 cm^{-1} measured for the b-Si coated with 20-nm thick Ag and Au films. Note that the SERS spectra and corresponding conversion results for Ag/b-Si was obtained irradiation intensity of 13.1 $\mu W/\mu m^2$, while for Au-coated b-Si - at higher intensity of 120 $\mu W/\mu m^2$.

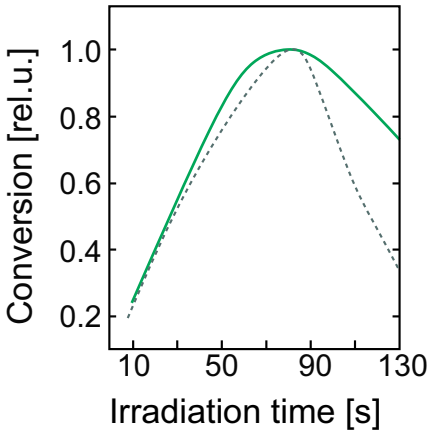

Figure 5: PATP-to-DMAB conversion measured for dried PATP layer on the b-Si coated with 100-nm thick Ag film (solid curve) in comparison to the measurement on the same substrate in the PATP aqueous methanol solution (dashed curve).